



Supplement of

SO₂ and NH₃ emissions enhance organosulfur compounds and fine particle formation from the photooxidation of a typical aromatic hydrocarbon

Zhaomin Yang et al.

Correspondence to: Lin Du (lindu@sdu.edu.cn)

The copyright of individual parts of the supplement might differ from the article licence.

S1. Size-dependent wall loss correction method

In the present work, the size-dependent particle wall-loss rate constants were determined based on the SMPS-measured particle size distribution. The first-order loss rate constants (k_i) of particles in each size bin i across all measured sizes were firstly calculated as the slope of the corresponding ln-linear fit line:

$$\ln[M_i(t)] = -k_i t + C \quad (S1)$$

where M_i ($\mu\text{g m}^{-3}$) is the mass concentration of particles in size bin i at time t (min) and C is an arbitrary constant. Then, the relationship between the k_i and the particle diameter ($d_{p,i}$) can be described as follows:

$$k_i(d_{p,i}) = ad_{p,i}^b + cd_{p,i}^{-d} \quad (S2)$$

The optimized fitted line shown in Fig. S1 can express well our independent seed experimental results. Parameters a , b , c , and d in Eq. (S2) were determined to be 5.5×10^{-6} , 1.05, 0.18, 1.19, respectively. Therefore, the size-dependent loss rate (k) of ammonium sulfate particles can be expressed as $k = 5.5 \times 10^{-6} \times d_p^{1.05} + 0.18 \times d_p^{-1.19}$.

S2. The formed H₂SO₄ estimation and inorganic mixture experiments

In order to evaluate the SO₂ effects on SOA formation, we used the method of Ye et al. (2018) to calculate the contribution of the generated H₂SO₄ to the particle formation enhancement in TMB/NO_x/SO₂ photooxidation (Ye et al., 2018; Wyche et al., 2009), where we assumed the conversion of the consumed SO₂ into H₂SO₄ aerosol particles. The contribution of the formed H₂SO₄ to the increase in particle volume concentration was less than 100 % (Fig. S6), demonstrating that the enhanced SOA formation is also responsible for the increased particle volume concentration. Additionally, a previous study has shown that half of the reacted SO₂ can transform into sulfur-containing organic species during the photooxidation of 1,3,5-trimethylbenzene/o-xylene/octane/toluene (Vivanco et al., 2011). HRMS measurements revealed the OSs production in this work, which may result in the decrease in the amount of H₂SO₄ in the particle phase. Therefore, the enhancement in aerosol particles by SO₂ introduction cannot be solely attributed to inorganic aerosol formation. Pure SO₂ oxidation experiments without introducing TMB were also carried out. In the TMB/NO_x/SO₂ regime, the consumption of 9.9 and 23.3 ppb SO₂ could cause the particle

volume concentration to increase by 32.9 and 89.2 $\mu\text{m}^3 \text{cm}^{-3}$, respectively. However, in pure SO_2 oxidation experiments, the volume concentrations of the formed particles were only 25.3 and 43.2 $\mu\text{m}^3 \text{cm}^{-3}$ when the consumptions of SO_2 were 9.5 and 24.2 ppb, respectively. Comparison of the results of TMB/ NO_x / SO_2 and pure SO_2 oxidation experiments also demonstrates that the enhancement in aerosol particles by SO_2 introduction cannot be solely attributed to inorganic aerosol formation.

Table S1. Particle parameters for experiments 1–8.

Exp.	Nucleation time (min)	Particle mean diameter (nm)	Initial particle growth rate (nm h⁻¹)
1	70	125.5	46.53
2	15	109.9	20.09
3	10	121.2	27.42
4	10	130.6	31.09
5	100	123.1	23.51
6	20	118.5	19.30
7	10	112.4	22.14
8	10	136.5	29.82

Table S2. Summary of characteristic wavenumbers of selected functional groups.

Functional groups	Absorption frequencies (cm⁻¹)	References
organic nitrates (RONO ₂)	860, 1280, 1630–1640	(Bruns et al., 2010)
sulfates (SO ₄ ²⁻)	612–615, 1103–1135	(Hawkins et al., 2010)
aliphatic carbon (C-H)	2850–3000	(Zhong and Jang, 2014)
esters (RC(O)OR')	1050–1160	(Hung et al., 2013)
O-O	960	(Jia and Xu, 2018)
C-N stretch	1315	(Liu et al., 2015)
carboxylic acids (RC(O)OH)	875–970, 1210–1320, 1685–1740, 2500–3300	(Hung et al., 2013)
aldehydes (RC(O)H)	1325–1450, 1720–1740	(Hung et al., 2013)
ketones (RC(O)R')	1100–1170, 1715–1745	(Hung et al., 2013)
alcohols (R-OH)	3200–3500	(Zhong and Jang, 2014)

Table S3. Compounds detected in aerosol particles from TMB/NO_x and TMB/NO_x/SO₂ photooxidation using UPLC-HRMS.

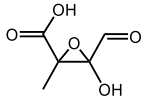
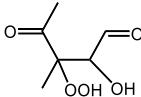
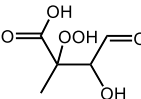
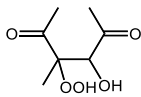
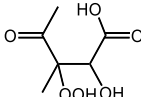
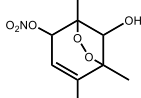
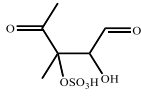
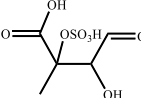
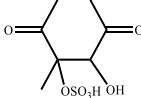
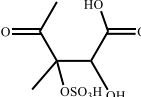
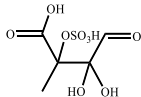
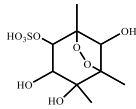
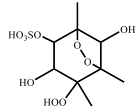
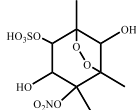
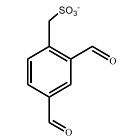
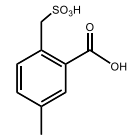
Molecular weight	Measured [M - H] ⁻	Suggested ion formula	Error (ppm) ^c	Retention times (min)	Proposed chemical structure ^d
146 ^{a, b}	145.01418	C ₅ H ₅ O ₅ ⁻	-0.490	3.59	
162 ^{a, b}	161.04555	C ₆ H ₉ O ₅ ⁻	-0.468	3.89, 4.63, 4.99	
164 ^{a, b}	163.02481	C ₅ H ₇ O ₆ ⁻	-0.751	3.14	
176 ^{a, b}	175.06091	C ₇ H ₁₁ O ₅ ⁻	-1.620	17.77	
178 ^{a, b}	177.04030	C ₆ H ₉ O ₆ ⁻	-0.919	2.35, 8.80	
231 ^{a, b}	230.06656	C ₉ H ₁₂ O ₆ N ⁻	-1.962	17.68, 15.03	
Organosulfates					
226 ^b	225.00772	C ₆ H ₉ O ₇ S ⁻	1.219	4.10, 5.11	
228 ^b	227.00150	C ₅ H ₇ O ₈ S ⁻	-2.059	20.48, 20.67	
240 ^b	239.02271	C ₇ H ₁₁ O ₇ S ⁻	-1.638	6.39, 7.76, 8.70	
242 ^b	241.00168	C ₆ H ₉ O ₈ S ⁻	-2.833	3.61, 4.21	
244 ^b	242.99619	C ₅ H ₇ O ₉ S ⁻	-2.886	12.98, 13.30	

Table S3. Continued.

Molecular weight	Measured [M - H] ⁻	Suggested ion formula	Error (ppm) ^c	Retention times (min)	Proposed chemical structure ^d
300 ^b	299.04395	C ₉ H ₁₅ O ₉ S ⁻	-0.938	3.56, 11.29, 11.85	
316 ^b	315.03867	C ₉ H ₁₅ O ₁₀ S ⁻	-1.494	7.23	
345 ^b	344.02853	C ₉ H ₁₄ O ₁₁ NS ⁻	-2.250	9.70	
214 ^b	212.98590	C ₈ H ₅ O ₅ S ⁻	-1.954	15.04	Unidentified
268 ^b	267.01724	C ₈ H ₁₁ O ₈ S ⁻	-2.879	10.41	Unidentified
Organic sulfonates					
228 ^b	227.00159	C ₉ H ₇ O ₅ S ⁻	-1.675	20.51, 20.68	
230 ^b	229.01706	C ₉ H ₉ O ₅ S ⁻	-2.437	22.66, 22.94, 23.39	

^a The products were observed in the TMB/NO_x photooxidation.

^b The products were detected in the TMB/NO_x/SO₂ photooxidation.

^c The molecular formula was assigned based on accurate mass measurements with a mass tolerance of ± 5 ppm.

^d Only one possible isomer was shown here.

Table S4. Observed $C_cH_hO_oN_n$ products in both SO_2 -free and SO_2 -involved experiments with NH_3 addition.

Molecular weight	Measured ions	Suggested ion formula	Error (ppm) ^c	Retention times (min)	O/C	$\log_{10}C^*$ ($\mu g\ m^{-3}$) ^d
74 ^a	72.99308	$C_2HO_3^-$	-0.508	2.20	1.50	6.16
88 ^a	87.00876	$C_3H_3O_3^-$	-0.100	3.02	1.00	6.18
150 ^a	149.0088	$C_4H_5O_6^-$	-1.882	2.35	1.50	2.16
114 ^a	113.02439	$C_5H_5O_3^-$	-0.231	9.65, 10.62	0.60	5.87
146 ^a	145.01407	$C_5H_5O_5^-$	-1.277	3.61	1.00	3.53
162 ^a	161.00876	$C_5H_5O_6^-$	4.311	2.78, 2.89	1.20	2.23
148 ^a	147.02985	$C_5H_7O_5^-$	-0.342	3.19	1.00	3.53
164 ^a	163.02470	$C_5H_7O_6^-$	-0.657	3.12	1.20	2.23
174 ^a	173.00879	$C_6H_5O_6^-$	4.188	3.34	1.00	2.20
128 ^a	127.04013	$C_6H_7O_3^-$	0.497	14.71, 15.13	0.50	5.61
144 ^a	143.03482	$C_6H_7O_4^-$	-1.128	7.64,9.12, 11.53	0.67	4.58
160 ^a	159.03011	$C_6H_7O_5^-$	1.314	9.34, 10.15, 12.77	0.83	3.43
176 ^a	175.02451	$C_6H_7O_6^-$	4.520	4.20	1.00	2.20
146 ^a	145.05052	$C_6H_9O_4^-$	-0.759	8.80	0.67	4.58
162 ^a	161.04543	$C_6H_9O_5^-$	-0.753	3.87, 4.63, 4.98, 5.94	0.83	3.43
178 ^a	177.04028	$C_6H_9O_6^-$	-1.005	2.35, 8.79	1.00	2.20
172 ^a	171.02988	$C_7H_7O_5^-$	-0.116	6.63, 11.07,12.96	0.71	3.28
188 ^a	187.02446	$C_7H_7O_6^-$	3.985	12.18	0.86	2.11
156 ^a	157.05048	$C_7H_9O_4^-$	-0.993	10.14, 11.11, 16.53	0.57	4.36
174 ^a	173.04514	$C_7H_9O_5^-$	-2.376	5.64, 7.98, 9.91, 14.54	0.71	3.28
190 ^a	189.03993	$C_7H_9O_6^-$	3.003	3.70, 4.17, 8.33	0.86	2.11
160 ^a	159.06609	$C_7H_{11}O_4^-$	-1.234	14.35	0.57	4.36
176 ^a	175.06070	$C_7H_{11}O_5^-$	-2.840	17.77	0.71	3.28
216 ^a	215.01923	$C_8H_7O_7^-$	-2.324	9.96	0.88	0.79
186 ^a	185.04509	$C_8H_9O_5^-$	-2.469	12.62	0.63	3.08
202 ^a	201.04025	$C_8H_9O_6^-$	4.418	7.12, 12.36	0.75	1.97
188 ^a	187.06075	$C_8H_{11}O_5^-$	-2.413	11.10, 11.84, 12.87	0.63	3.08
204 ^a	203.05577	$C_8H_{11}O_6^-$	3.724	11.78, 12.20,	0.75	1.97
184 ^a	185.08040	$C_9H_{13}O_4^+$	-2.360	13.98, 16.27	0.44	3.81
216 ^a	215.05579	$C_9H_{11}O_6^-$	-1.512	13.38, 16.76	0.67	1.79
232 ^a	231.05043	$C_9H_{11}O_7^-$	2.169	12.67,14.10, 19.52	0.78	0.66
202 ^a	201.07658	$C_9H_{13}O_5^-$	-1.307	24.32	0.56	2.85
218 ^a	217.07117	$C_9H_{13}O_6^-$	2.314	16.44	0.67	1.79
234 ^a	233.06613	$C_9H_{13}O_7^-$	-2.336	11.06, 11.78	0.78	0.66
250 ^a	249.06107	$C_9H_{13}O_8^-$	-2.107	12.43	0.89	-0.53

Table S4. Continued.

Molecular weight	Measured ions	Suggested ion formula	Error (ppm) ^c	Retention times (min)	O/C	log ₁₀ C* (μg m ⁻³) ^d
250 ^a	249.06107	C ₉ H ₁₃ O ₈ ⁻	-2.107	12.43	0.89	-0.53
220 ^a	219.08690	C ₉ H ₁₅ O ₆ ⁻	-2.339	21.26	0.67	1.79
236 ^a	235.08188	C ₉ H ₁₅ O ₇ ⁻	-1.903	3.91, 4.34	0.78	0.66
252 ^a	251.07664	C ₉ H ₁₅ O ₈ ⁻	-2.372	3.63	0.89	-0.53
229 ^a	228.05083	C ₉ H ₁₀ O ₆ N ⁻	-2.338	10.19, 11.96	0.67	0.36
229 ^b	230.06591	C ₉ H ₁₂ O ₆ N ⁺	-3.365	25.17	0.67	0.36
231 ^a	230.06701	C ₉ H ₁₂ O ₆ N ⁻	-2.028	14.57, 15.01, 17.69	0.67	0.36
231 ^b	232.08087	C ₉ H ₁₄ O ₆ N ⁺	-2.981	9.43, 11.78	0.67	0.36
265 ^a	264.07187	C ₉ H ₁₄ O ₈ N ⁻	-2.350	18.69	0.89	-1.09
265 ^b	266.08615	C ₉ H ₁₆ O ₈ N ⁺	-3.351	17.14	0.89	-1.09
191 ^a	190.03529	C ₆ H ₈ O ₆ N ⁻	-2.192	2.65	1.00	1.36

^a The molecules were detected by UPLC-HRMS in the negative mode.

^b The molecules were detected by UPLC-HRMS in the positive mode.

^c The molecular formula was assigned based on accurate mass measurements with a mass tolerance of ± 5 ppm.

^d The saturation mass concentrations of observed products were predicted based on the method of Li et al. (2016).

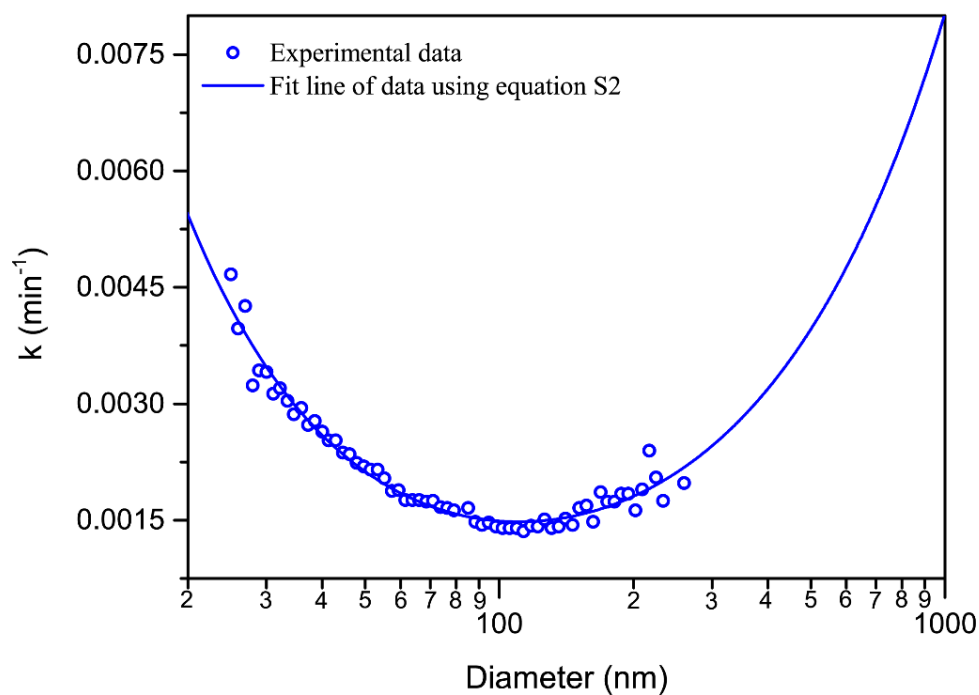


Figure S1. Wall loss rate constant of particles as a function of particle diameter.

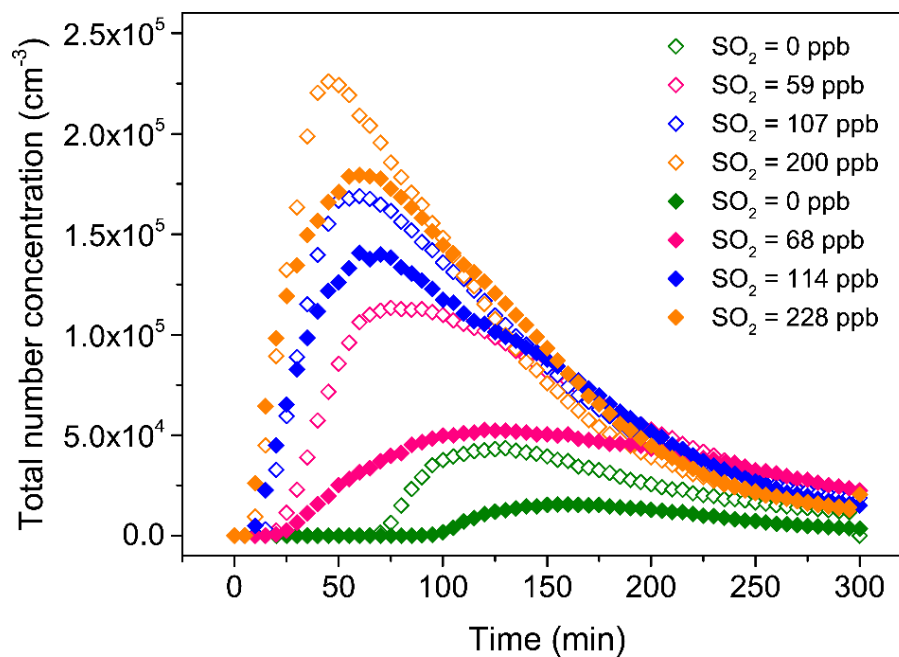


Figure S2. The total number concentrations of ultrafine particles (< 100 nm) as a function of reaction time (Exps. 1–8). The open symbols and solid symbols represent low- and high- NO_x experiments, respectively.

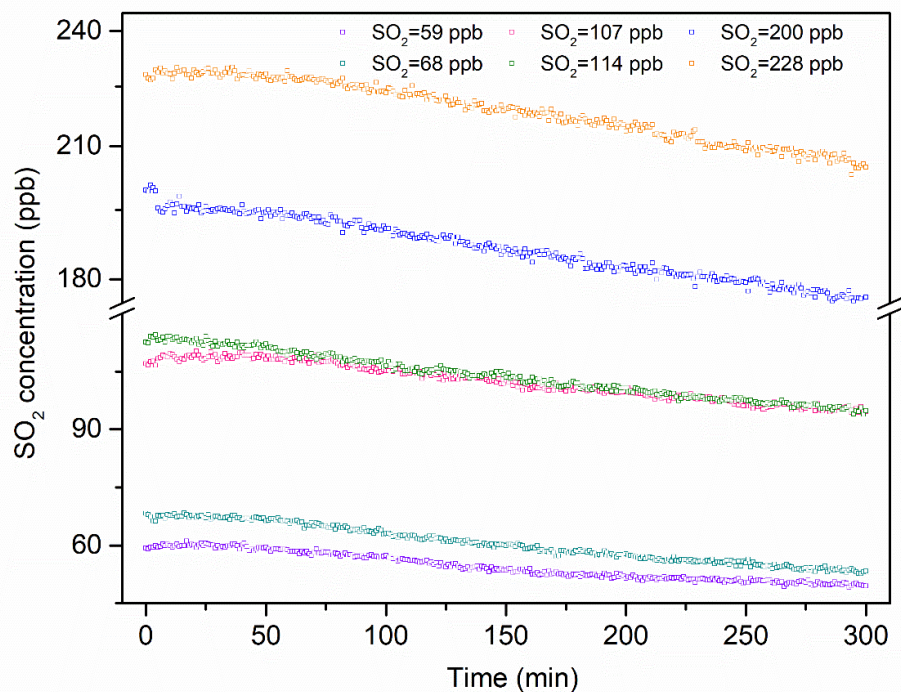


Figure S3. Decay of SO₂ during the photooxidation of TMB (Exps. 2–4, 6–8).

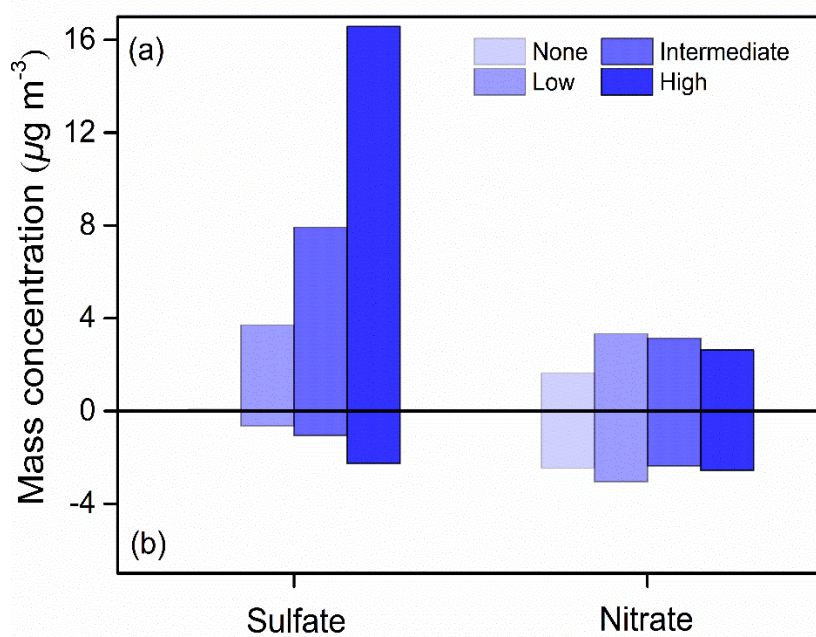


Figure S4. The particle sulfate and nitrate loadings for aerosol samples collected from the photooxidation of TMB under low- (a) and high-NO_x (b) conditions with SO₂ introduction. None: SO₂ = 0 ppb; low: SO₂ = 50–70 ppb intermediate: SO₂ = 100–120 ppb; high: SO₂ = 200–230 ppb.

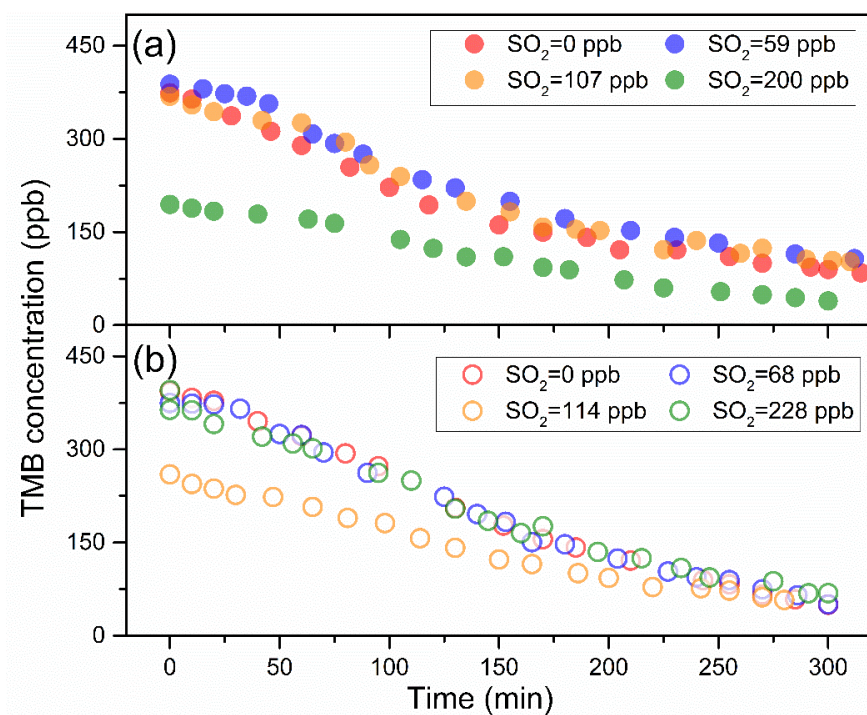


Figure S5. Time profiles of TMB for photooxidation experiments under low- (a) and high-NO_x (b) conditions with different SO₂ levels.

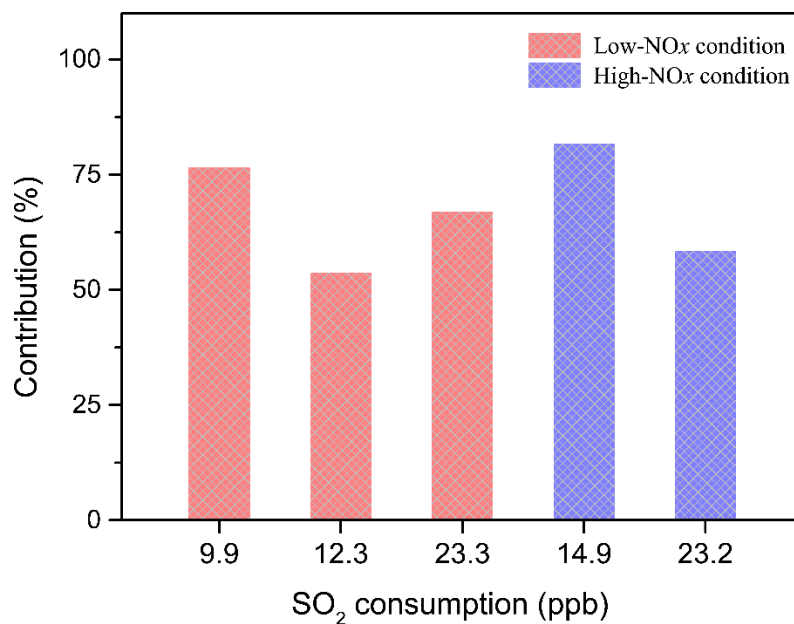


Figure S6. Contribution (%) of the formed H₂SO₄ to the increased particle volume concentration during low-NO_x and high-NO_x experiments.

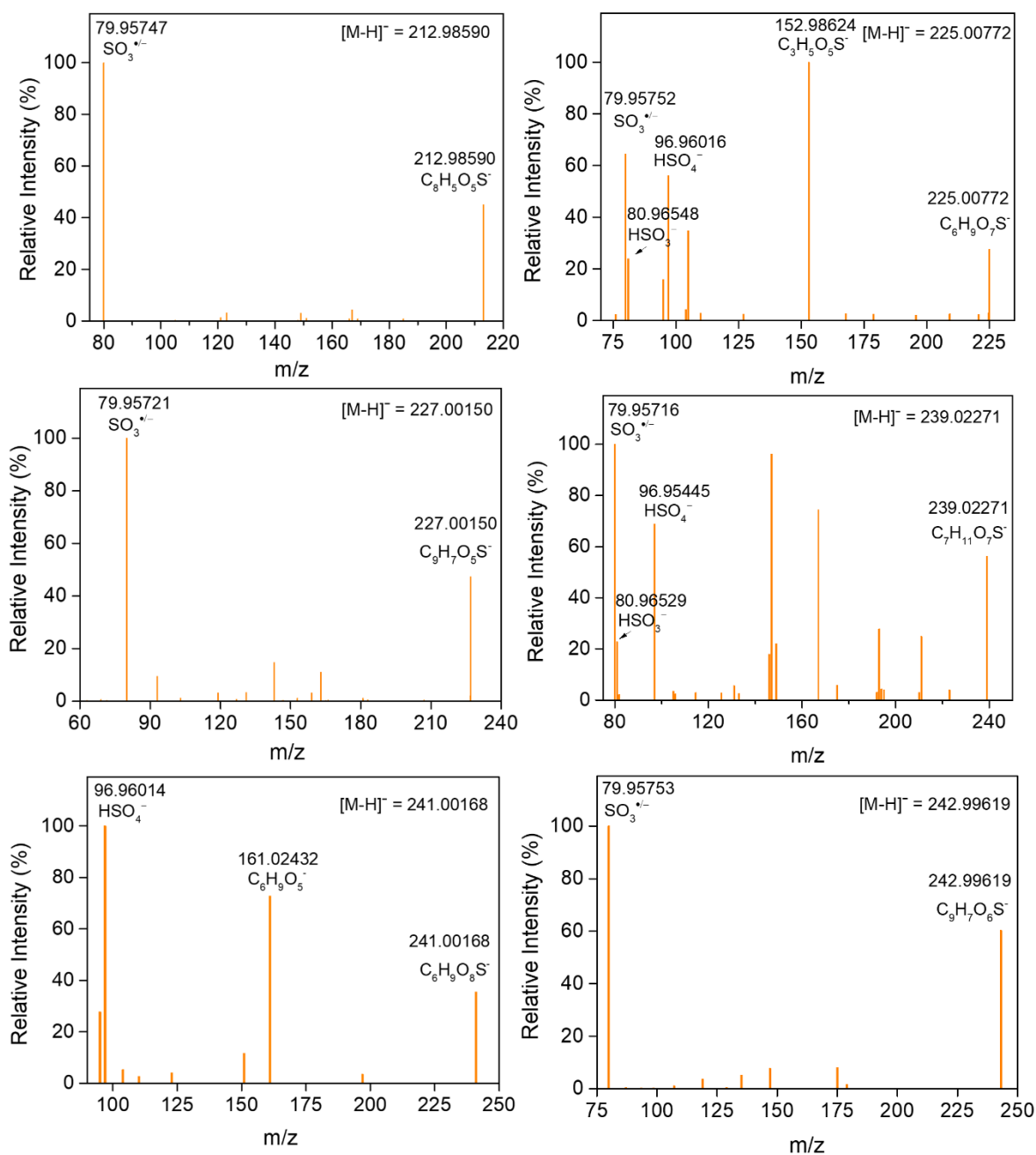


Figure S7. MS/MS spectra of organosulfates generated from the photooxidation of TMB in the presence of SO₂.

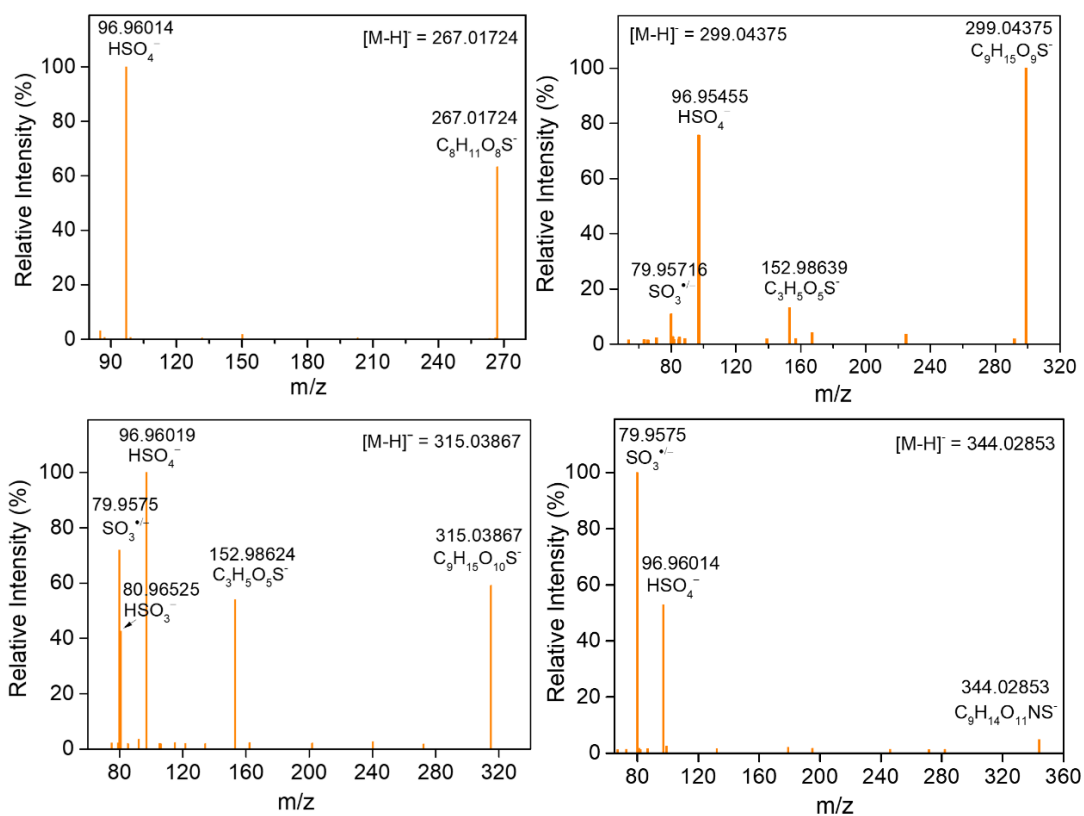


Figure S7. Continued.

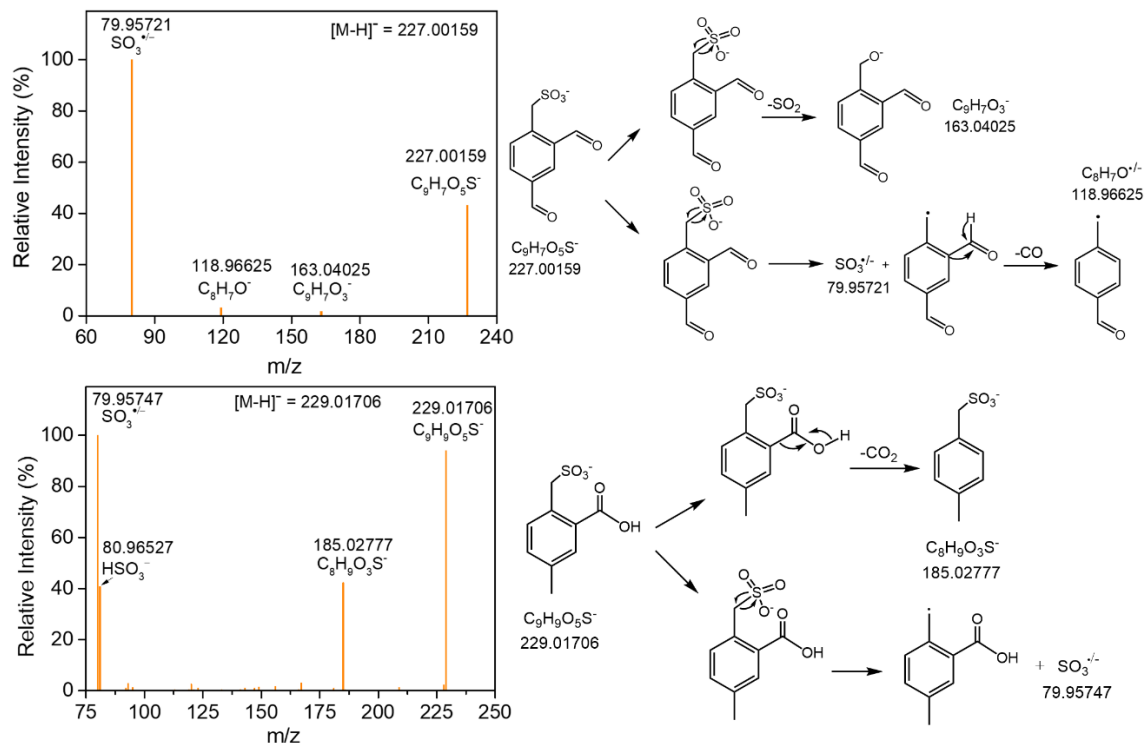


Figure S8. MS/MS spectra and fragmentation schemes of ion at m/z 227.00159 and 229.01706 observed in aerosol particles from TMB photooxidation in the presence of SO_2 .

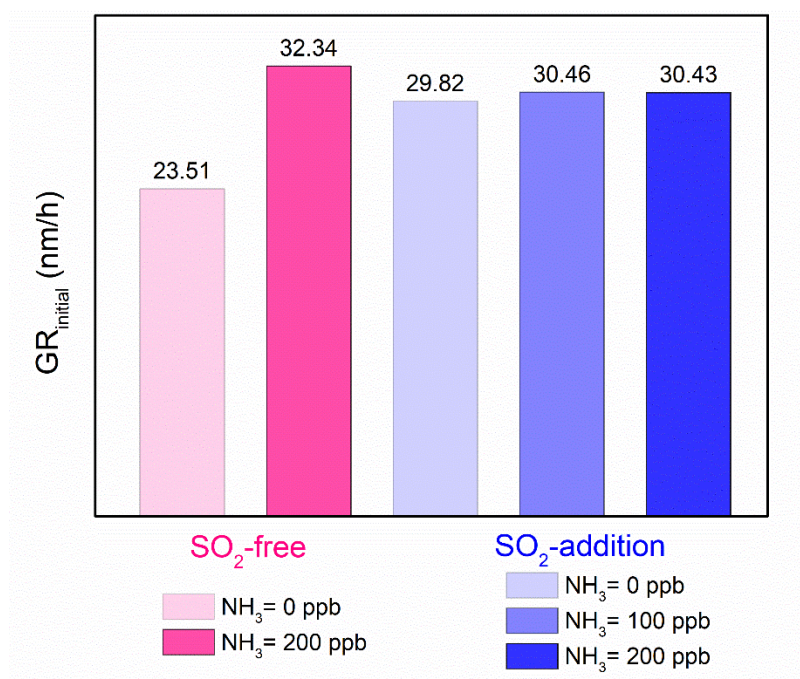


Figure S9. Observed initial growth rates of aerosol particles under SO_2 -free and SO_2 -added (~ 230 ppb) conditions (Exps. 5, 8, 10–12).

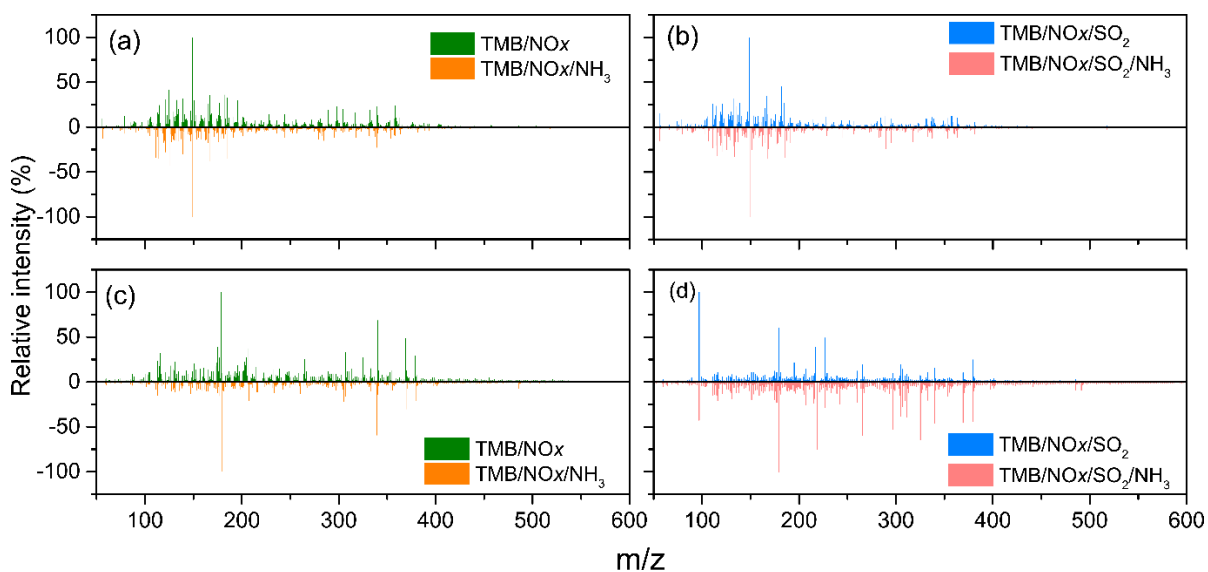


Figure S10. High-resolution mass spectra of aerosol particles from TMB photooxidation with/without NH_3 introduction. Panels a–b: positive ion mode. Panels c–d: negative ion mode.

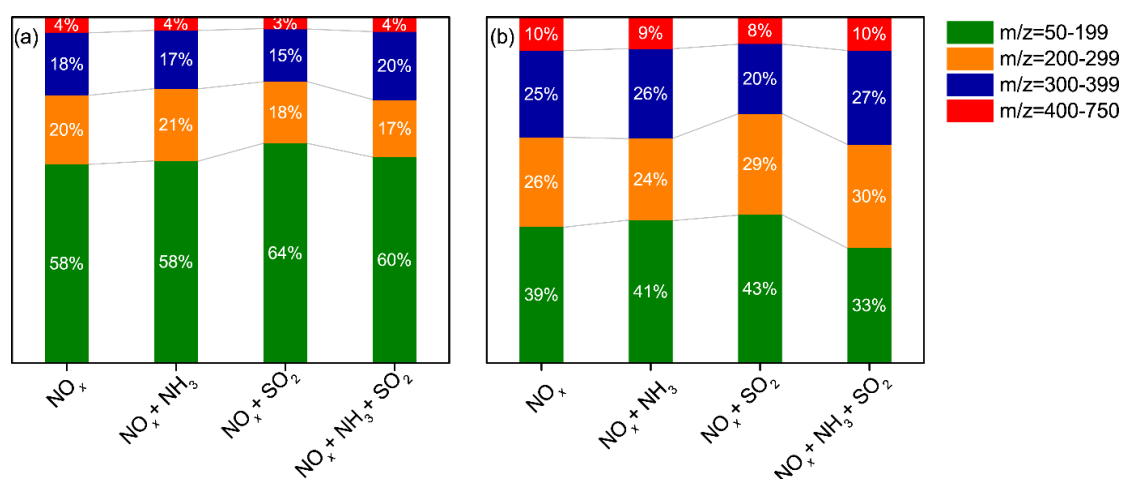


Figure S11. Relative contributions (% by abundance) of ions detected by UPLC-HRMS in the positive mode (a) and negative mode (b) for aerosol particles collected from different experiments (Exps. 5, 8, 10, 12).

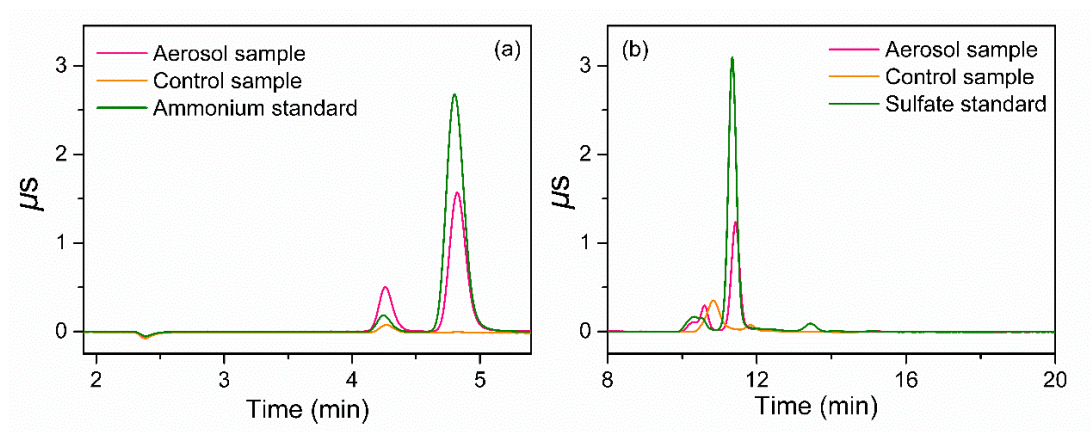


Figure S12. Ion chromatography results for aerosol particles formed from the photooxidation of TMB in the presence of SO₂ and NH₃. Panel (a): Ammonium. Panel (b): Sulfate

References

- Bruns, E. A., Perraud, V., Zelenyuk, A., Ezell, M. J., Johnson, S. N., Yu, Y., Imre, D., Finlayson-Pitts, B. J., and Alexander, M. L.: Comparison of FTIR and particle mass spectrometry for the measurement of particulate organic nitrates, *Environ. Sci. Technol.*, 44, 1056-1061, 10.1021/es9029864, 2010.
- Hawkins, L. N., Russell, L. M., Covert, D. S., Quinn, P. K., and Bates, T. S.: Carboxylic acids, sulfates, and organosulfates in processed continental organic aerosol over the southeast Pacific Ocean during VOCALS-REx 2008, *J. Geophys. Res.*, 115, D13201, 10.1029/2009jd013276, 2010.
- Hung, H. M., Chen, Y. Q., and Martin, S. T.: Reactive aging of films of secondary organic material studied by infrared spectroscopy, *J. Phys. Chem. A*, 117, 108-116, 10.1021/jp309470z, 2013.
- Jia, L., and Xu, Y.: Different roles of water in secondary organic aerosol formation from toluene and isoprene, *Atmos. Chem. Phys.*, 18, 8137-8154, 10.5194/acp-18-8137-2018, 2018.
- Li, Y., Pöschl, U., and Shiraiwa, M.: Molecular corridors and parameterizations of volatility in the chemical evolution of organic aerosols, *Atmos. Chem. Phys.*, 16, 3327-3344, 10.5194/acp-16-3327-2016, 2016.
- Liu, Y., Liggitto, J., Staebler, R., and Li, S. M.: Reactive uptake of ammonia to secondary organic aerosols: kinetics of organonitrogen formation, *Atmos. Chem. Phys.*, 15, 13569-13584, 10.5194/acp-15-13569-2015, 2015.
- Vivanco, M. G., Santiago, M., Martinez-Tarifa, A., Borrás, E., Rodenas, M., Garcia-Diego, C., and Sanchez, M.: SOA formation in a photoreactor from a mixture of organic gases and HONO for different experimental conditions, *Atmos. Environ.*, 45, 708-715, 10.1016/j.atmosenv.2010.09.059, 2011.
- Wyche, K. P., Monks, P. S., Ellis, A. M., Cordell, R. L., Parker, A. E., Whyte, C., Metzger, A., Dommen, J., Duplissy, J., Prevot, A. S. H., Baltensperger, U., Rickard, A. R., and Wulfert, F.: Gas phase precursors to anthropogenic secondary organic aerosol: detailed observations of 1,3,5-trimethylbenzene photooxidation, *Atmos. Chem. Phys.*, 9, 635-665, 10.5194/acp-9-635-2009, 2009.
- Ye, J., Abbatt, J. P. D., and Chan, A. W. H.: Novel pathway of SO₂ oxidation in the atmosphere: reactions with monoterpene ozonolysis intermediates and secondary organic aerosol, *Atmos. Chem. Phys.*, 18, 5549-5565, 10.5194/acp-18-5549-2018, 2018.
- Zhong, M., and Jang, M.: Dynamic light absorption of biomass-burning organic carbon photochemically aged under natural sunlight, *Atmos. Chem. Phys.*, 14, 1517-1525, 10.5194/acp-14-1517-2014, 2014.